Conformational Analysis of [D-Ala^9]α-Factor and [L-Ala^9]α-Factor in Solution and in the Presence of Lipid†

J. S. Gounarides,‡ M. S. Broido,‡,§ J. M. Becker,∥ and F. R. Naider*,⊥

Department of Chemistry, Hunter College and The Graduate School of the City University of New York, 695 Park Avenue, New York, New York 10021, Department of Microbiology, University of Tennessee, Knoxville, Tennessee 37996, and Department of Chemistry, College of Staten Island and The Graduate School of the City University of New York, 130 Stuyvesant Place, Staten Island, New York 10301

Received July 30, 1992; Revised Manuscript Received November 13, 1992

ABSTRACT: The conformations in solution and in the presence of lipid vesicles of [D-Ala^9] and [L-Ala^9] analogues of the α-factor (WHWLQLKPGQPMY) from the yeast *Saccharomyces cerevisiae* were examined by NMR spectroscopy. Although both peptides are flexible molecules, NOE and NH dδ/dT data indicate that the [D-Ala^9]α-factor analogue in DMSO and aqueous solution adopts a type II β-turn about residues 8 and 9. In contrast, various NMR parameters for the less active [L-Ala^9] analogue do not provide evidence for a regular secondary structure in solution. Transfer NOE data indicate that for both peptides binding to the lipid is strongest for the N-terminal residues. The C-terminus of the [D-Ala^9] analogue appears to be more constrained in the bound state than the C-terminus of the [L-Ala^9] analogue. This result is consistent with transfer NOE evidence that the type II β-turn conformation of the [D-Ala^9]α-factor is maintained in the lipid bound state.

The α-factor of the yeast *Saccharomyces cerevisiae* is a tridecapeptide mating pheromone with the sequence Trp^1-His^2-Trp^3-Leu^4-Gln^5-Leu^6-Lys^7-Pro^8-Gly^9-Gln^{10}-Pro^{11}-Met^{12}-Tyr^{13}. The pheromone is secreted by α-mating type cells (MATα) and initiates a series of hormone-like responses in MATa cells in preparation for sexual conjugation. These include an increase in cell surface agglutinins and the cessation of DNA synthesis in the G-1 phase of the growth cycle (Thorner, 1980).

Jelicks et al. (1988) reported that, although the α-factor is a highly flexible molecule in both DMSO[1] and aqueous solution, the pheromone adopts a transient type II β-turn centered about Pro^8 and Gly^9. It was also found that the α-factor interacted with lipid vesicles and that the peptide maintained the β-turn conformation upon binding to the lipid vesicles (Jelicks et al., 1989).

We have found that the [D-Ala^9]α-factor has an activity comparable to that of the native pheromone, while the [L-Ala^9] analogue is 10-fold less active. It was anticipated that the activities of these two analogues were related to their different conformational preferences. On the basis of both theoretical and experimental precedent (Venkatachalam, 1968; Rose et al., 1985) the substitution of D-alanine for glycine in α-factor would be expected to favor a type II β-turn conformation, whereas substitution with L-alanine is expected to destabilize this conformation. The conformation of a peptide in the membrane-bound state may be significantly different from that in solution (Wu et al., 1982; Higashijima et al., 1983; Wakamatsu et al., 1986a; Milon et al., 1990). Significantly, for analogues of enkephalin (Milon et al., 1990) and luteinizing hormone releasing hormone (Wakamatsu et al., 1986a) biological activity has been correlated with the membrane-bound conformation rather than with the conformations in solution. Therefore, we were interested in examining the conformation of the [D-Ala^9]- and [L-Ala^9]α-factor analogues both in solution and bound to unilamellar lipid vesicles. These tridecapeptides were chosen over dodecapeptide α-factor analogues [such as des-Trp^1 [Cha^3,Ala^9]α-factor which had been previously studied in DMSO-d_6 (Jelicks et al., 1988)] on the basis of considerations of retention times on C_{18} reversed-phase columns. The additional Trp residue makes the tridecapeptides appreciably more hydrophobic than homologous dodecapeptides (Shenbagamurthi and Naider, unpublished results). Thus, it was anticipated that the tridecapeptides would interact more strongly than dodecapeptides with lipid vesicles. In this paper we report results of a detailed analysis of the solution and lipid-bound conformation of the [D-Ala^9]- and [L-Ala^9]α-factors using one- and two-dimensional NMR spectroscopy.

MATERIALS AND METHODS

Peptides were synthesized as described by Tallon et al. (1987). Peptide purity was checked by reversed-phase HPLC using an acetonitrile/water/trifluoroacetic acid gradient and was determined to be greater than 97%. The purified peptides had the expected amino acid ratios, and no extraneous peaks were observed in the NMR spectra of these compounds. Chain-perdeuterated L-α-dipalmitoylphosphatidylcholine (DPPC-d_{62}) was purchased from Cambridge Isotope Laboratories (CIL) and was used without further purification.

For studies of the peptides in solution, samples were 2.0–2.5 mM peptide in DMSO-d_6 (100%, CIL) or 4.0 mM peptide in 90% H_2O/10% D_2O (CIL). The pH of aqueous samples was adjusted to 4.6 (the pH of the yeast culture medium) using dilute (100 mM) stock solutions of NaOH or HCl. The

† This work was supported by NIH Grants GM22086 and GM22087 and a grant from the PSC–CUNY Research Award Program.

‡ Hunter College.

§ Present address: National Institute of General Medical Sciences, 5333 Westbard Ave., Bethesda, MD 20892.

∥ University of Tennessee.

⊥ College of Staten Island.

[1] Abbreviations: DMSO, dimethyl sulfoxide; DPPC, L-α-dipalmitoylphosphatidylcholine; EDTA, ethylenedinitrotetraacetic acid; 1-D, one dimensional; 2-D, two dimensional; DQF-COSY, 2-D double quantum filtered correlated spectroscopy; NOE, nuclear Overhauser effect; NOESY, 2-D NOE spectroscopy; ROESY, rotating frame Overhauser spectroscopy; TRNOE, transfer NOE; TRNOESY, 2-D transfer NOE spectroscopy; dδ/dT, temperature coefficient.

0006-2960/93/0432-908$04.00/0

pH was not corrected for isotope effect. Lipid vesicles were prepared in 5 mM sodium acetate buffer (pH 4.6, 10% D_2O, 50 μM EDTA) by low-power sonication as described by Jelicks et al. (1989). Two-dimensional transfer NOE (TRNOESY) experiments (Clore & Gronenborn, 1982; Glaudemans et al., 1990; Campbell & Sykes, 1991) were run on samples containing either 8 mM DPPC/4 mM peptide or 8 mM DPPC/2 mM peptide.

The high degree of curvature of sonicated vesicles has led some investigators to question whether the packing of the phospholipid molecule in a vesicle is similar to that found in biological membranes (Sheetz & Chan, 1972; Chan et al., 1973). The lipid-phase transition temperature, T_c, is expected to be very sensitive to the packing of the phospholipid molecules. de Kruijff et al. (1975) have reported that the T_c for lipid dispersions and sonicated vesicles of the same composition are not significantly different, and we have measured a T_c of 41 °C for both DPPC dispersions and sonicated DPPC vesicles using DSC (Naider et al., 1989). Therefore, we believe that sonicated phospholipid vesicles are a reasonable model for a biological membrane.

NMR spectroscopy was performed on the 400-MHz (^1H) JEOL GX-400 spectrometer of the CUNY NMR facility located at Hunter College. Data processing was performed off-line on the μ-VAX of the RCMI Computer Graphics Facility using the FTNMR-51 package (Hare Research). Chemical shifts are reported relative to the residual proton resonance of DMSO at 2.49 ppm (DMSO samples) or to the H_2O signal at 4.78 ppm at 25 °C (aqueous samples). Selective saturation was used for the suppression of the H_2O signal. For spectra of aqueous samples the center of the spectrum was set to the frequency of the water resonance to remove images from imperfect quadrature detection. Setting the carrier frequency to that of the water resonance also reduced the possibility of coherent magnetization transfer between the amide and α-protons in ROESY spectra (Bax & Davis, 1985). The spin-locking field for ROESY experiments was 3.1 kHz.

All spectra were accumulated at 25 °C unless otherwise stated. At 25 °C the DPPC vesicles are in the gel state and might be expected to interact differently with the peptide pheromones than would the liquid crystalline phase, which more closely simulates the cell membrane. We have attempted to measure the TRNOESY spectra of the [D-Ala^9]- and the [L-Ala^9]α-factor at 45 °C, which is slightly above the T_c of DPPC. At this temperature both peptides exhibited a high degree of spectral overlap in the NH–αCH region. Furthermore, the intensity of the NH–αCH connectivities was reduced due to partial saturation from the irradiation used to suppress the water resonance. In a previous study by Jelicks et al. (1989) few cross-peaks were reported for spectra measured on α-factor in the presence of DPPC vesicles at 41 °C. Given the above difficulties and the results of Jelicks et al. (1989), we only carried out a detailed TRNOE analysis at 25 °C. However, we believe that it is likely that the conformations of the [D-Ala^9]- and [L-Ala^9]α-factors are similar regardless of whether the lipid vesicles are in the gel phase or in the liquid crystalline phase.

DQF-COSY (Rance et al., 1983), NOESY (Macura & Ernst, 1980), and ROESY (Bax & Davis, 1985) spectra were recorded using the method of States et al. (1982) with 2048 complex points in t_2, 384 t_1 increments, and postacquisition delays of 2.0 s. DQF-COSY spectra in all solvents and NOESY spectra of DMSO solution samples were collected with 32 acquisitions per t_1 increment. NOESY and ROESY spectra run on the peptides in aqueous solution were collected with 64 acquisitions per t_1 increment. TRNOESY experiments were performed using the standard NOESY pulse sequence, which was not equipped to remove signals arising from zero-quantum coherence. TRNOESY spectra were collected with 256 t_1 increments and 32 acquisitions per t_1 increment. Absolute value COSY spectra were collected with 256 t_1 increments and were used for the measurement of amide temperature coefficients. In all cases the t_1 dimension was zero-filled to obtain a 1K by 1K spectrum of real data.

Mixing times of 100, 200, and 400 ms were used for NOESY experiments performed on samples in DMSO. For the peptides in aqueous solution a 400-ms mixing time and a 250-ms spin-lock time were used for NOESY and ROESY experiments, respectively. For the TRNOESY experiments a 75-ms mixing time was used.

NOESY spectra were processed using a $\pi/2$ shifted squared-sine bell multiplication in both time dimensions. For ROESY spectra a skewed $\pi/2$ shifted sine-squared bell was applied in both time dimensions. A cubic spline baseline correction was applied to the F_2 dimension of all NOESY and ROESY spectra, and in addition a fourth-order polynomial baseline correction was applied to the F_1 dimension of TRNOESY spectra. The method of Otting et al. (1985) was used for the reduction of t_1 ridges.

RESULTS

Assignments. Proton resonance assignments (Tables I and II) were made by the identification of amino acid spin systems in the DQF-COSY spectrum. Side-chain resonances which did not show connectivities in the DQF-COSY spectrum (i.e., His^2 C_2H and C_4H, Gln^5 γNH_2, Gln^{10} γNH_2, and Met^{12} SCH_3) were assigned by analysis of 1-D spectra and intraresidue NOESY connectivities. Sequential NOEs were used to discriminate between replicated spin systems, and intraresidue NOEs were used to distinguish between the two tryptophan aromatic spin systems (Wüthrich, 1986). The assignments made in the present study for the [D-Ala^9]- and [L-Ala^9]α-factor support those made on the α-factor by Jelicks et al. (1988) with the exception of those of the backbone and β-proton resonances of His^2 and Trp^3, which should be interchanged. This reversal is also supported by NMR studies on the [^{2}H-Trp^3]α-factor (M. Tallon, personal communication).

Conformational Analysis in Aqueous Solution. For both peptides Lys^7-Pro^8 and Gln^{10}-Pro^{11} αCH_i–δCH_{i+1} NOE connectivities were observed (data not shown), indicating that these peptide bonds are predominantly trans (Wüthrich, 1986). No evidence for a cis proline bond, as indicated by additional resonances or by the presence of a αCH–αCH NOE connectivity, was observed for either the [D-Ala^9]- or [L-Ala^9]α-factors. This result is consistent with the findings of Jelicks et al. (1988) on the native α-factor.

The NH_i–NH_{i+1} and αCH_i–NH_{i+1} NOE connectivities for both peptides under all experimental conditions are summarized in Figure 1. All αCH_i–NH_{i+1} NOE connectivities were observed in the NOESY and ROESY spectra of the [D-Ala^9] analogue in aqueous solution. Prominent features of the NOESY and ROESY spectra of the [D-Ala^9]α-factor (Figure 2) in water are the very strong cross-peak between the Pro^8 αCH and the Ala^9 NH protons and the very weak Ala$^9{}_{\alpha CH}$–Gln$^{10}{}_{NH}$ NOE connectivity. Only two other sequential αCH–NH NOE connectivities in the NOESY spectrum (Figure 2A), the His$^2{}_{\alpha CH}$–Trp$^3{}_{NH}$ and Met$^{12}{}_{\alpha CH}$–Tyr$^{13}{}_{NH}$ cross-peaks, have intensities as weak as that of the Ala$^9{}_{\alpha CH}$–Gln$^{10}{}_{NH}$ connectivity. Both the His^2-Trp^3 and Met^{12}-Tyr^{13} residue

Table I: ^{1}H Assignments for [D-Ala^9]α-Factor in DMSO (D) and in Water (W)

residue		NH	αCH	βCH	γCH	δCH	εCH	other
Trp^1	D		4.05	3.15 2.97				ring protons 7.58, 6.80, 7.01, 7.32, 7.15, indole NH 10.92
	W		4.21	3.21 3.14				ring protons 7.49, 7.05, 7.21, 7.48, 7.06, indole NH 10.03
His^2	D	8.86	4.65	3.02				C_2H 8.99 C_4H 7.31
	W		4.56	3.08 2.97				C_2H 8.42 C_4H 7.10
Trp^3	D	8.27	4.61	3.17 2.98				ring protons 7.66, 6.97, 7.05, 7.32, 7.16, indole NH 10.82
	W	8.05	4.54	3.26 3.16				ring protons 7.63, 7.16, 7.20, 7.43, 7.24, indole NH 10.12
Leu^4	D	8.49	4.35	1.46	1.59	0.85		
	W	8.17	4.25	1.52	1.52	0.88[a] 0.81		
Gln^5	D	8.05	4.27	1.76	2.11			γNH_2 7.32,[a] 6.81, 7.30, 6.84
	W	8.17	4.25	2.00 1.90	2.29			γNH_2 7.52, 6.86
Leu^6	D	7.84	4.30	1.38	1.57	0.79		
	W	8.24	4.34	1.64 1.56	1.52	0.88[a] 0.81		
Lys^7	D	8.08	4.44	1.50	1.34	1.50	2.75	ϵNH_3 7.63
	W	8.22	4.60	1.78 1.64	1.42	1.67	2.96	ϵNH_3
Pro^8	D		4.27	2.05	1.86	3.69 3.50		
	W		4.32	2.27	2.07 1.99	3.81[a] 3.80 3.65 3.61		
D-Ala^9	D	8.19	4.23	1.19				
	W	8.60	4.32	1.39				
Gln^{10}	D	7.88	4.42	1.88 1.73	2.10			γNH_2 7.32,[a] 6.81, 7.30, 6.84
	W	7.96	4.60	2.10 1.98	2.36			γNH_2 7.52, 6.86
Pro^{11}	D		4.34	2.00	1.90	3.62		
	W		4.37	2.19 1.78	2.06 1.99	3.81[a] 3.80 3.65 3.61		
Met^{12}	D	8.03	4.31	1.86 1.73	2.42 2.39			S-CH_3 2.00
	W	8.26	4.32	1.91 1.84	2.47 2.38			S-CH_3 2.03
Tyr^{13}	D	7.97	4.32	2.93 2.77				$C_{2,6}H$ 6.99 $C_{3,5}H$ 6.64
	W	7.53	4.40	3.08 2.87				$C_{2,6}H$ 7.08 $C_{3,5}H$ 6.79

[a] These resonances could not be assigned to individual residues of duplicated amino acids.

Table II: ^{1}H Assignments for [L-Ala^9]α-Factor in DMSO (D) and in Water (W)

residue		NH	αCH	βCH	γCH	δCH	εCH	other
Trp^1	D		4.03	3.13 2.95				ring protons 7.57, 6.78, 6.99, 7.31, 7.14, indole NH 10.91
	W		4.21	3.21 3.14				ring protons 7.50, 7.07, 7.22, 7.48, 7.07, indole NH 10.04
His^2	D	8.86	4.67	3.03				C_2H 8.96 C_4H 7.32
	W		4.56	3.09 2.99				C_2H 8.41 C_4H 7.11
Trp^3	D	8.27	4.62	3.16 2.96				ring protons 7.67, 6.97, 7.04, 7.31, 7.16, indole NH 10.81
	W	8.05	4.52	3.26 3.16				ring protons 7.63, 7.18, 7.22, 7.43, 7.25, indole NH 10.14
Leu^4	D	8.41	4.35	1.43	1.60	0.83		
	W	8.14	4.24	1.51	1.44	0.88 0.81		
Gln^5	D	8.06	4.27	1.84	2.09			γNH_2 7.29,[a] 6.79, 7.24, 6.74
	W	8.18	4.21	2.01 1.93	2.27			γNH_2 7.55,[a] 6.88, 7.52, 6.86
Leu^6	D	7.92	4.28	1.39	1.54	0.80		
	W	8.23	4.32	1.62	1.58	0.91 0.85		
Lys^7	D	7.97	4.42	1.61 1.48	1.31	1.50	2.73	ϵNH_3 7.63
	W	8.26	4.57	1.78	1.42	1.67	2.98	ϵNH_3
Pro^8	D		4.31	1.95 1.72	1.87 1.79	3.64 3.46		
	W		4.36	2.29 1.91	2.02 1.99	3.77[a] 3.59 3.67		
L-Ala^9	D	7.98	4.17	1.15				
	W	8.38	4.26	1.37				
Gln^{10}	D	7.90	4.45	1.85 1.64	2.09			γNH_2 7.29,[a] 6.79, 7.24, 6.74
	W	8.19	4.60	2.09 1.92	2.36			γNH_2 7.55,[a] 6.88, 7.52, 6.86
Pro^{11}	D		4.29	2.00	1.85 1.79	3.64		
	W		4.34	2.20 1.78	2.02 1.97	3.77[a] 3.67 3.59		
Met^{12}	D	7.99	4.30	1.85 1.74	2.42 2.38			S-CH_3 2.01
	W	8.30	4.37	1.98 1.88	2.48 2.36			S-CH_3 2.08
Tyr^{13}	D	7.99	4.30	2.91 2.76				$C_{2,6}H$ 6.98 $C_{3,5}H$ 6.63
	W	7.64	4.41	3.13 2.88				$C_{2,6}H$ 7.11 $C_{3,5}H$ 6.83

[a] These resonances could not be assigned to individual residues of duplicated amino acids.

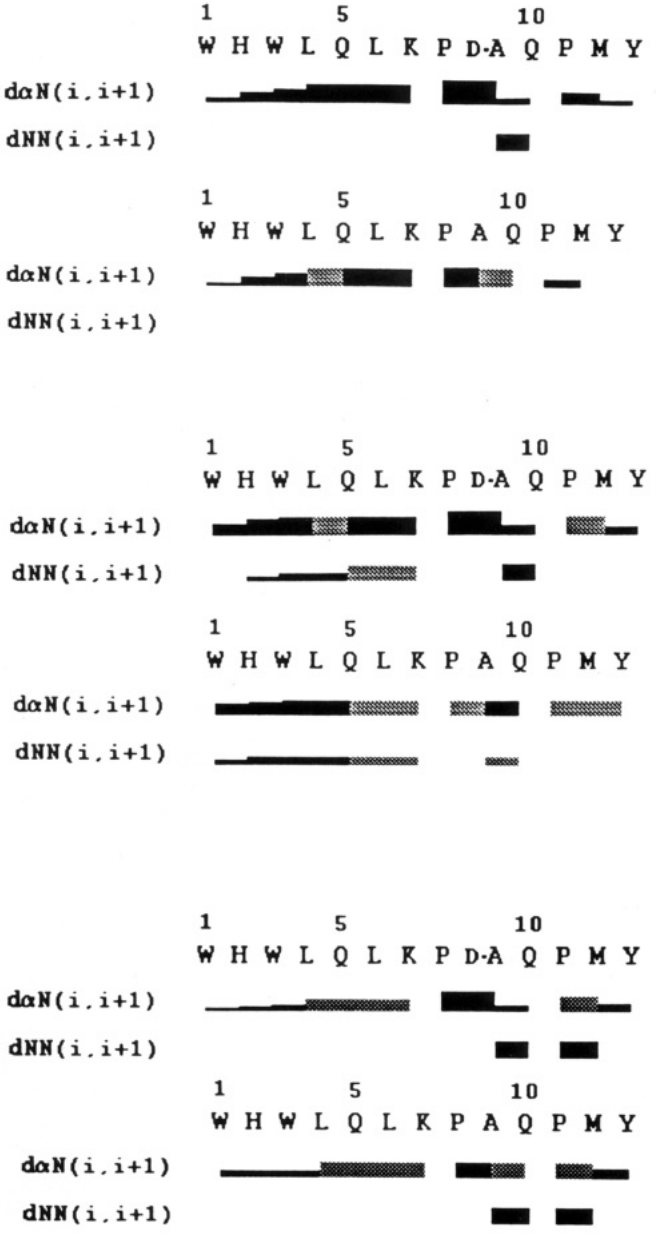

FIGURE 1: Summary of sequential NOESY connectivities for the [D-Ala^9]- and [L-Ala^9]α-factor in (A, top) water (pH 4.6), (B, middle) DMSO, and (C, bottom) in the presence of DPPC vesicles. The diagram indicates the relative strength of the cross-peak by differences in height. Regions of spectral overlap are indicated by a cross-hatched gray designation.

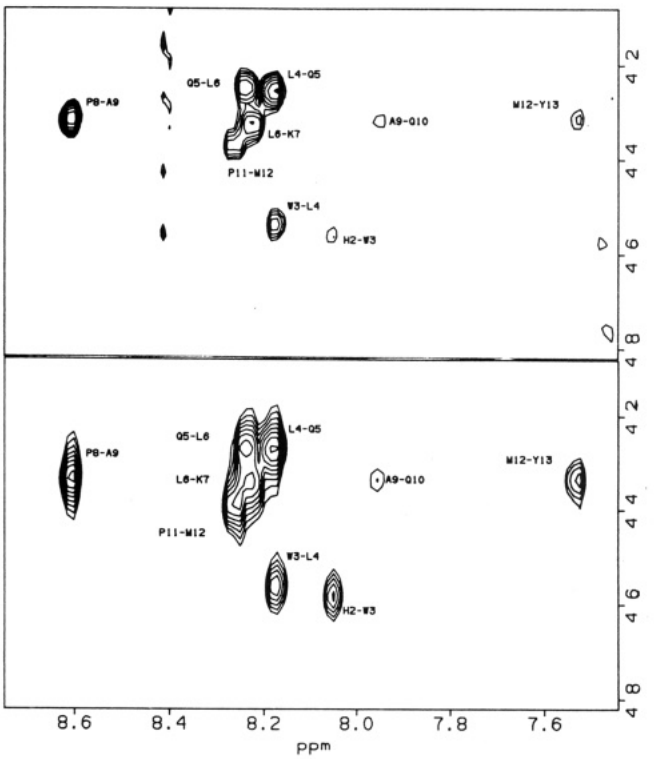

FIGURE 2: αCH–NH region of the (A, top) 400-ms NOESY spectrum and (B, bottom) 250-ms ROESY spectrum of the [D-Ala^9]α-factor in water.

pairs are located at the termini of the molecule and are likely to experience shorter correlation times (τ_c) than central residue pairs. They are, therefore, expected to exhibit weaker NOE intensities than residues in the center of the mating factor (Balaram, 1985; Wüthrich, 1986). In the ROESY spectrum (Figure 2B), where short correlation time effects are less significant, both the His$^2{}_{\alpha CH}$–Trp$^3{}_{NH}$ and the Met$^{12}{}_{\alpha CH}$–Tyr$^{13}{}_{NH}$ cross-peaks significantly increase in intensity, while the Ala$^9{}_{\alpha CH}$–Gln$^{10}{}_{NH}$ cross-peak intensity remains weak.

The strong intensity of the Pro$^8{}_{\alpha CH}$–Ala$^9{}_{NH}$ cross-peak and the weak intensity of the Ala$^9{}_{\alpha CH}$–Gln$^{10}{}_{NH}$ NOE connectivity are consistent with a type II β-turn centered about the Pro^8 and D-Ala^9 residues (Balaram, 1985; Wüthrich, 1986; Dyson et al., 1988). A nonsequential αCH_{i+1}–NH_{i+3} NOE connectivity between Pro^8 and Gln^{10} would be expected for a β-turn structure (Wüthrich, 1986; Dyson et al., 1988). Such a cross-peak, however, was not observed. If present, this cross-peak would be obscured due to spectral overlap with the Ala$^9{}_{\alpha CH}$–Gln$^{10}{}_{NH}$ connectivity. No attempt was made to observe the Pro$^8{}_{\alpha CH}$–Gln$^{10}{}_{NH}$ cross-peak by α-deuteration of the Ala^9 residue as it was anticipated that the Pro$^8{}_{\alpha CH}$–Gln$^{10}{}_{NH}$ interaction (with an internuclear distance of approximately 3.3 Å) would be below the detection limit at the peptide concentrations available to us. The Ala^9–Gln^{10} NH–NH connectivity is the only NH–NH connectivity observed in either the ROESY or NOESY spectrum of the [D-Ala^9]α-factor (Figure 3A) and provides further support for the presence of the β-turn suggested by the Pro$^8{}_{\alpha CH}$–Ala$^9{}_{NH}$ and Ala$^9{}_{\alpha CH}$–Gln$^{10}{}_{NH}$ cross-peaks.

In contrast to the [D-Ala^9] analogue, no NH–NH cross-peaks are observed in either the NOESY or ROESY spectrum of the [L-Ala^9]α-factor analogue in aqueous solution (Figure 3B). Furthermore, in the NOESY and ROESY spectra of the [L-Ala^9]α-factor (Figure 4) none of the αCH_i–NH_{i+1} connectivities have unusually strong or weak intensities. This, combined with the absence of NH–NH cross-peaks, suggests the absence of a highly populated conformation involving residues 7–10 which contain a β-turn.

In the 400-ms NOESY spectrum of the [L-Ala^9]α-factor (Figure 4B) the Met$^{12}{}_{\alpha CH}$–Tyr$^{13}{}_{NH}$ cross-peak is absent, indicating that this interaction has a shorter effective correlation time than all other αCH_i–NH_{i+1} NOE connectivities (Balaram, 1985; Wüthrich, 1986). The apparently higher degree of freedom of the C-terminus of the [L-Ala^9] analogue is consistent with this peptide being less structured than the [D-Ala^9]α-factor analogue (Allerhand & Oldfield, 1973).

Conformational Analysis in DMSO Solution. As in water, αCH_i–δCH_{i+1} NOE connectivities were observed between Lys^7-Pro^8 and Gln^{10}-Pro^{11} in both the [D-Ala^9]- and [L-Ala^9]α-factor analogues in DMSO (data not shown). Despite spectral overlap, all of the αCH_i–NH_{i+1} NOE connectivities can be discerned for the [D-Ala^9]α-factor (Figure 5A). The Pro$^8{}_{\alpha CH}$–Ala$^9{}_{NH}$ cross-peak is again observed to be very strong, while

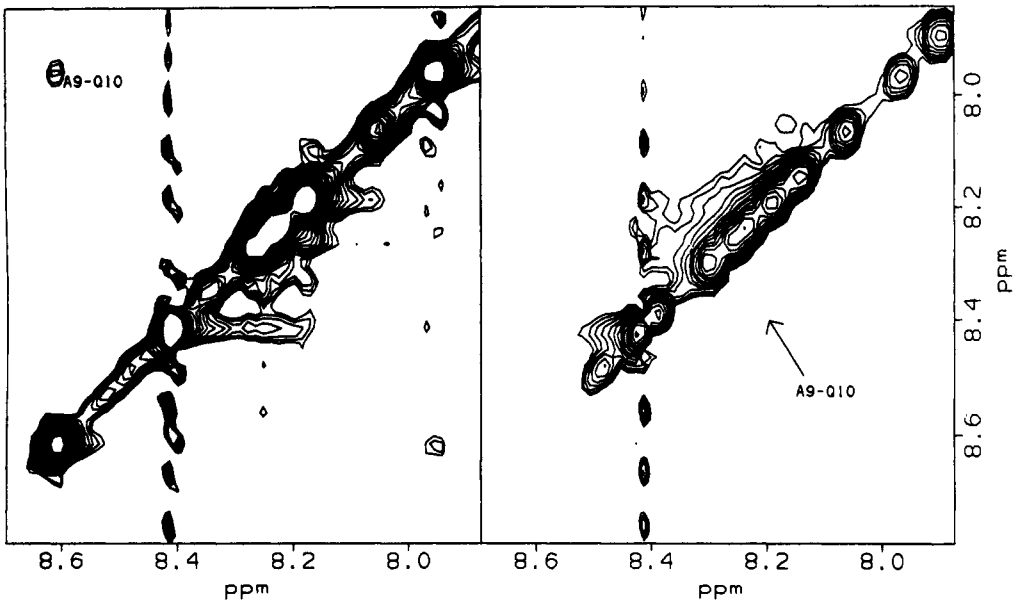

FIGURE 3: NH–NH region of the 400-ms NOESY spectrum of the (A, left) [D-Ala^9]α-factor and (B, right) [L-Ala^9]α-factor in water. Arrow indicates expected position of Ala^9$_{NH}$–Gln^{10}$_{NH}$ cross-peak.

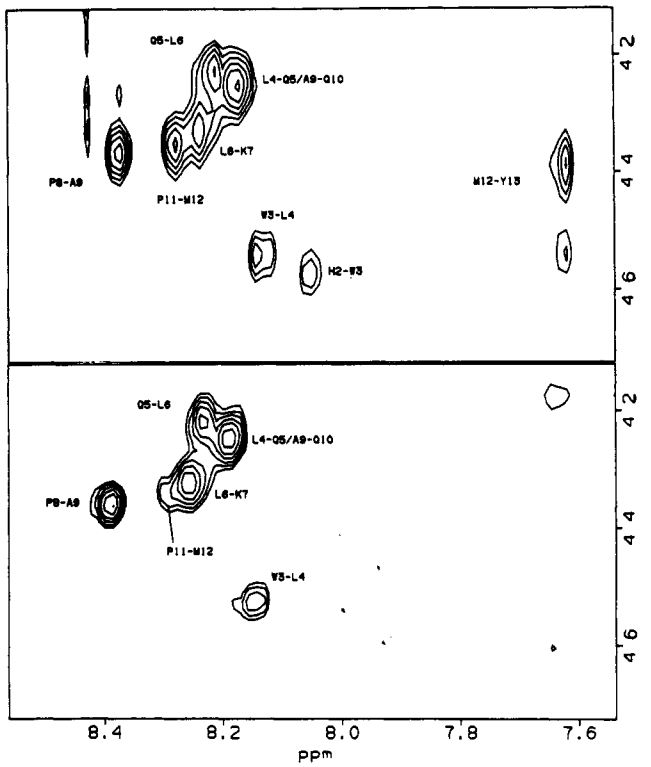

FIGURE 4: αCH–NH region of the (A, top) 250-ms ROESY spectrum and (B, bottom) 400-ms NOESY spectrum of the [L-Ala^9]α-factor in water.

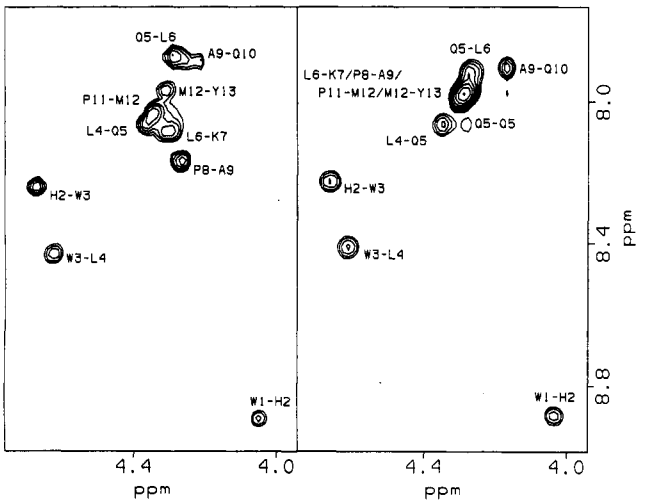

FIGURE 5: αCH–NH region of the 400-ms NOESY spectrum of the (A, left) [D-Ala^9]α-factor and (B, right) [L-Ala^9]α-factor in DMSO.

the Ala^9$_{\alpha CH}$–Gln^{10}$_{NH}$ connectivity is relativity weak, supporting the conclusion that residues 7–10 of the [D-Ala^9]α-factor adopt a type II β-turn in DMSO.

For the [L-Ala^9]α-factor the spectral overlap in the NOESY spectrum (Figure 5B) is more severe and the Leu^6-Lys^7, Pro^8-Ala^9, Pro^{11}-Met^{12}, and Met^{12}-Tyr^{13} αCH_i–NH_{i+1} NOE connectivities form a single, coalesced cross-peak. As can be seen in Figure 5B, the Ala^9$_{\alpha CH}$–Gln^{10}$_{NH}$ cross-peak in the [L-Ala^9]α-factor is very strong. The intensity of this cross-peak is stronger than would be expected if the Pro^8 and Ala^9 residues were involved in a β-turn (Wüthrich, 1986; Dyson et al., 1988).

All possible sequential NH–NH cross-peaks, except for the Met^{12}-Tyr^{13} NH–NH cross-peak, are observed in the NOESY spectra of both diastereomers (Figure 6). The Met^{12}-Tyr^{13} NH–NH connectivity would be hidden by the diagonal, if present. The absence of long-range NOE connectivities suggests that the observed NH–NH cross-peaks are associated with predominantly unstructured peptide segments (Wright et al., 1988). However, the intensity of the Ala^9-Gln^{10} NH–NH connectivity in the spectra of the [D-Ala^9]α-factor (Figure 6A) is significantly stronger than those of all other NH–NH cross-peaks and supports the presence of a type II β-turn conformation involving residues 7–10 of this analogue.

Temperature Coefficients and Coupling Constants. The temperature dependencies of the amide proton chemical shifts (NH $d\delta/dT$) were determined over the ranges 19–49 °C in DMSO and 10–38 °C in water (Table III). The Gln^{10} in the [D-Ala^9] analogue in water has a NH $d\delta/dT$ of –3.6 ppb/K. This is significantly lower than the NH $d\delta/dT$ exhibited by other residues in the [D-Ala^9] peptide and is less than half the magnitude of the $d\delta/dT$ for the corresponding resonance in the [L-Ala^9] peptide (–8.2 ppb/K). The relatively low Gln^{10} NH $d\delta/dT$ clearly indicates that this proton is solvent shielded to a large degree, presumably through intramolecular hydrogen

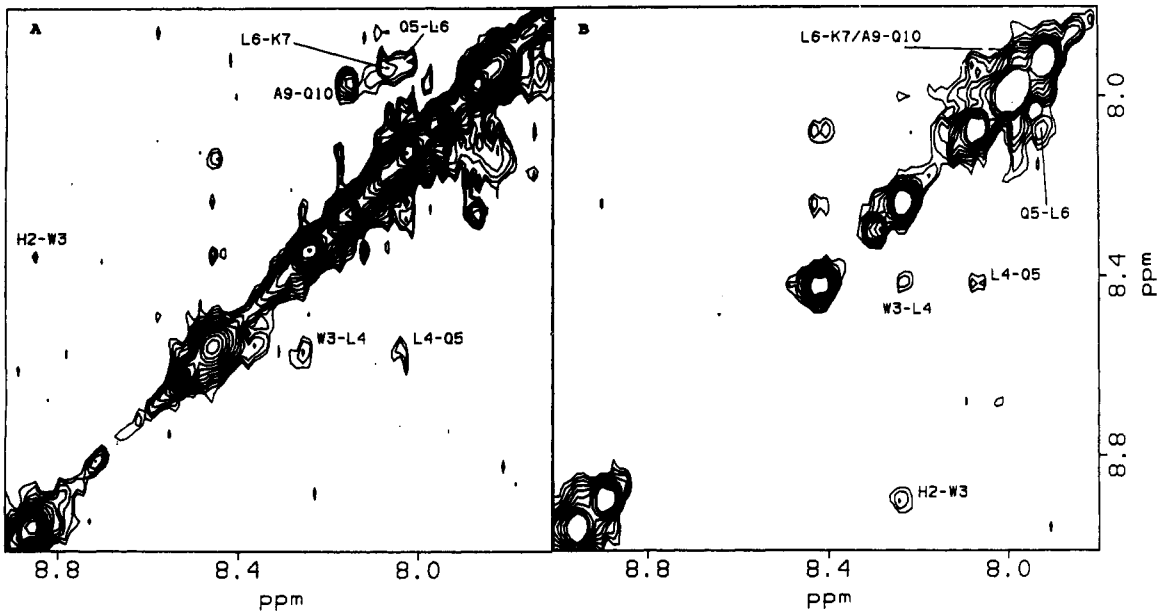

FIGURE 6: NH–NH region of the 400-ms NOESY spectrum of the (A) [D-Ala^9]α-factor and (B) [L-Ala^9]α-factor in DMSO.

Table III: Amide Proton Temperature Coefficients for α-Factor Analogue Peptides (in ppb/K)

	D-Ala^9		L-Ala^9	
NH	DMSO	water	DMSO	water
His^2	−4.3		−4.5	
Trp^3	−3.5	−7.3	−4.0	−7.5
Leu^4	−6.1	−5.9[a]	−6.6	−5.4
Gln^5	−4.0	−5.9[a]	−4.7	−5.5
Leu^6	−4.6	−8.6	−4.3	−8.2
Lys^7	−5.2	−7.0	−4.7	−7.7
Ala^9	−5.4	−8.0	−3.7	−8.2
Gln^{10}	−3.3	−3.6	−5.0	−8.2
Met^{12}	−4.2	−7.9	−6.2	−8.0
Tyr^{13}	−5.4	−4.3	−6.2	−5.7

[a] Resonances were overlapping.

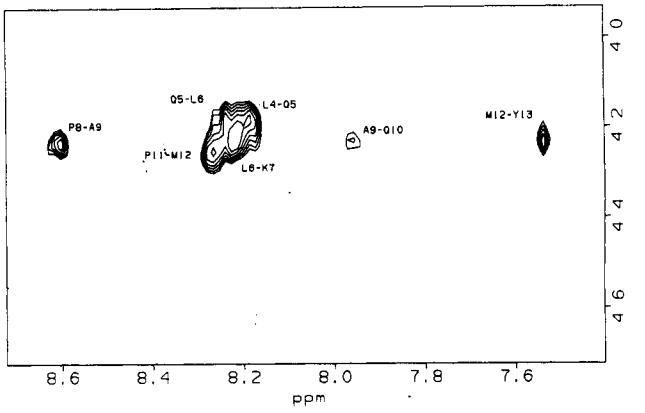

FIGURE 7: αCH–NH region of the 75-ms TRNOESY spectrum of the [D-Ala^9]α-factor. 8 mM DPPC/4 mM peptide.

bonding. As in water, the lowest NH $d\delta/dT$ of either peptide in DMSO is found for Gln^{10} of the [D-Ala^9]α-factor. However, the $d\delta/dT$ for the Gln^{10} NH resonance of the [D-Ala^9]α-factor analogue in DMSO (−3.3 ppb/K) is above the range which has been associated with strong hydrogen bonding in this solvent (Kessler, 1982; Balaram, 1985), and the difference between the NH temperature coefficients of the [L-Ala^9] and [D-Ala^9] homologues is smaller than that found in water.

Where $^3J_{\alpha NH}$ coupling constants could not be measured from high-resolution 1-D spectra, due to spectral overlap, they were estimated from DQF-COSY spectra zero-filled to a digital resolution of 1.38 Hz/point in the F_2 dimension. The $^3J_{\alpha NH}$ coupling constant of the [D-Ala^9]- and [L-Ala^9]α-factors in DMSO and in water are in the ranges 6.6–8.8 and 5.9–7.1, respectively. The $^3J_{\alpha NH}$ coupling constants indicate that both peptides are undergoing rapid conformational averaging (Kessler, 1982; Balaram, 1985).

α-Factor in the Presence of DPPC Vesicles. The ^{1}H resonances for both the [D-Ala^9] and [L-Ala^9] analogues broadened upon addition of lipid vesicles. However, the chemical shifts did not significantly change relative to those of the peptides in the absence of lipid vesicles. Similar results were obtained for enkephalin analogues (Milon et al., 1990) and the α-factor (Wakamatsu et al., 1986b; Jelicks et al., 1989) in the presence of lipid. Only one peak was observed for each peptide resonance, and the resonances sharpened with increasing temperature. One interpretation of these results is that the exchange rate is fast on the chemical shift time scale. This conclusion was confirmed by the results of 2-D transfer NOE (TRNOESY) experiments, the success of which depends on a fast exchange rate.

TRNOESY experiments were performed on samples of 8 mM DPPC/4 mM peptide and 8 mM DPPC/2 mM peptide. Unilamellar vesicles are expected to have an average rotational correlation time (τ_c) of approximately 10^{-6} rad s^{-1} (Stockton et al., 1976). Therefore, the spin–lattice relaxation and cross-relaxation rates of the peptide resonances will be strongly affected by interaction with lipid vesicles. Strong cross-peaks were observed in the 75-ms NOESY spectra of the α-factor analogues in the presence of DPPC vesicles (Figures 7 and 8). In contrast, the 75-ms NOESY spectra of the peptides in the absence of lipid vesicles were almost devoid of cross-peaks and those present were extremely weak (data not shown). The increase in NOE intensity in the presence of lipid indicated that the peptides interact with the lipid and that we are observing a TRNOE phenomenon (Clore & Gronenborn, 1982; Campbell & Sykes, 1991). This conclusion is supported by the relative changes observed for the relaxation parameters of residues at the N- and C-termini of the α-factor analogues (vide infra) as the [lipid]/[peptide] was increased.

Conformation of α-Factor Bound to DPPC Vesicles. In the TRNOESY spectrum of the [D-Ala^9] peptide in 8 mM DPPC, the Pro$^8{}_{\alpha CH}$-Ala$^9{}_{NH}$ TRNOESY cross-peak is very

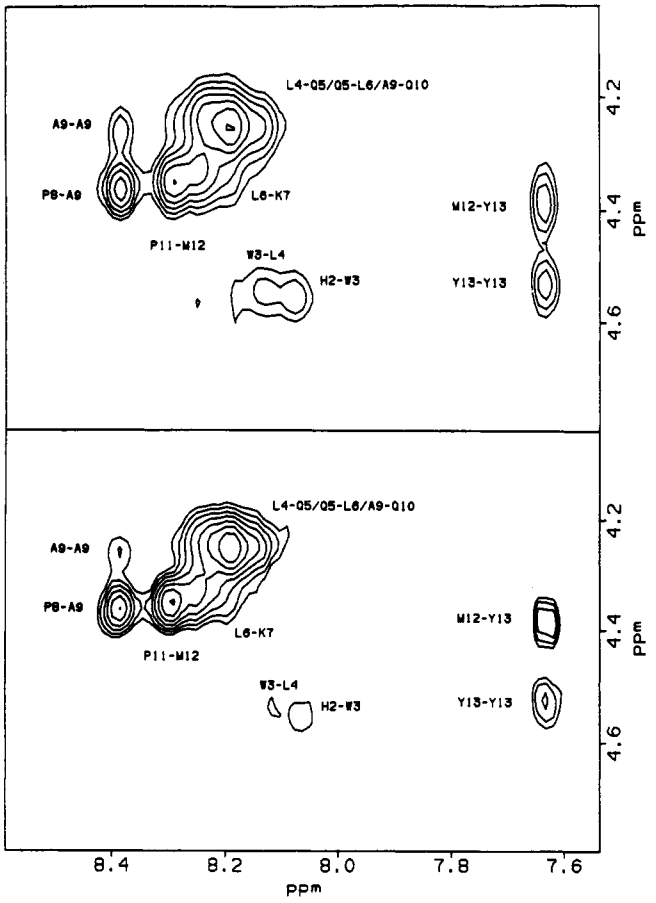

FIGURE 8: αCH–NH region of the 75-ms TRNOESY spectrum of the [L-Ala^9]α-factor. (A, top) 8 mM DPPC/4 mM peptide; (B, bottom) 8 mM DPPC/2 mM peptide.

strong and the Ala$^9{}_{\alpha CH}$–Gln$^{10}{}_{NH}$ TRNOESY cross-peak is weak (Figure 7). These results are consistent with the maintenance of the type II β-turn upon binding to lipid. No evidence for any other predominant conformational feature was observed in the TRNOESY spectra of this peptide. Little can be discerned concerning the lipid-bound conformation of the [L-Ala^9]α-factor analogue as many of the αCH_i–NH_{i+1} cross-peaks are broadened and form a single coalesced peak (Figure 8). For both peptides only the Ala^9-Gln^{10} and Met^{12}-Tyr^{13} NH–NH cross-peaks were visible in the NH–NH region of the TRNOESY spectra.

Peptide Binding to DPPC Vesicles. Figure 9 shows slices through the NH resonances of Trp^3 and Met^{12} in 75-ms NOESY spectra of the [L-Ala^9]α-factor in the presence and absence of lipid vesicles. As judged from the signal to noise ratio, the Trp^3 NH diagonal signal shows a greater decay rate with increased peptide binding relative to that of the Met^{12} NH diagonal. Diagonal signals in NOESY spectra decay with a rate equal to the selective spin–lattice relaxation rate, $1/T_1{}^s$ (Kumar et al., 1981; Mirau & Bovey, 1986). This parameter increases with $\tau_{c\ eff}$ and has been used for monitoring ligand binding (Valensin et al., 1982; Behling et al., 1988). The TRNOE can be used in an analogous manner. Specifically, the His$^2{}_{\alpha CH}$–Trp$^3{}_{NH}$ and Trp$^3{}_{\alpha CH}$–Leu$^4{}_{NH}$ TRNOE cross-peaks exhibited a marked decrease in intensity relative to the Tyr$^{13}{}_{\alpha CH}$–Tyr$^{13}{}_{NH}$ and Met$^{12}{}_{\alpha CH}$–Tyr$^{13}{}_{NH}$ TRNOE cross-peaks as the [lipid]/[peptide] ratio was increased (Figure 8). This decrease in intensity can be interpreted as the result of greater selective spin–lattice relaxation rates for Trp^3 and Leu^4 as compared to those for Met^{12} and Tyr^{13} and would be consistent with the N-terminus interacting more strongly with

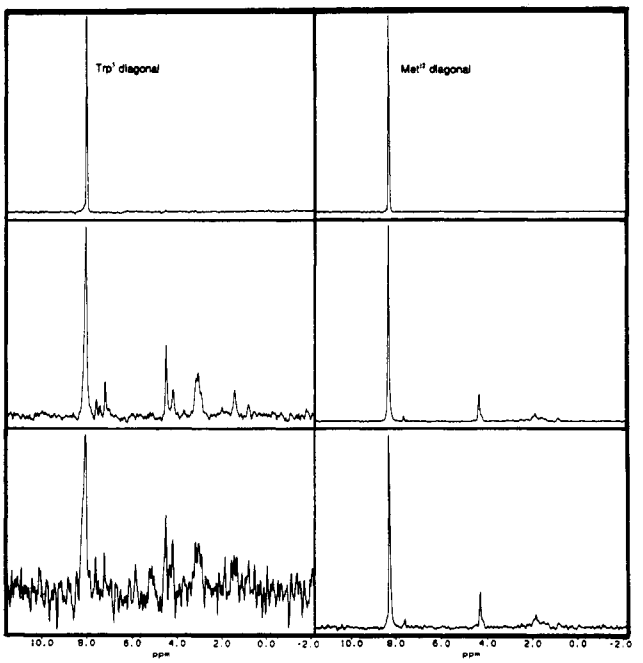

FIGURE 9: 1-D slices through the Trp^3 and Met^{12} NH resonances of the 75-ms TRNOESY spectra of the [L-Ala^9]α-factor. (A, top) Peptide in aqueous solution, no lipid present; (B, middle) 8 mM DPPC/4 mM peptide; (C, bottom) 8 mM DPPC/2 mM peptide.

the lipid than does the C-terminus of this peptide (Campbell & Sykes, 1991). This conclusion is in agreement with the findings of Wakamatsu et al. (1987) on α-factor.

In contrast to the result observed for the [L-Ala^9] analogue, the relative intensity of the Met$^{12}{}_{\alpha CH}$–Tyr$^{13}{}_{NH}$ cross-peak of the [D-Ala^9]α-factor does not increase with peptide binding. Rather, it disappears in the 8 mM DPPC/2 mM peptide spectrum (data not shown). The Tyr^{13} $C_{2,6}H$–$C_{3,5}H$ NOE cross-peak in the [D-Ala^9]α-factor increases to a greater extent relative to the Trp^1 and Trp^3 intra-ring NOE connectivities in the presence of DPPC vesicles than is found for the [L-Ala^9] analogue. Furthermore, distortions to this cross-peak due to the superposition of zero-quantum J cross-peaks (Macura et al., 1981, 1982) are less pronounced for the [D-Ala^9]α-factor than the [L-Ala^9]α-factor at corresponding peptide concentrations (data not shown). For both peptides the effects of *zero*-quantum coherence on the Tyr^{13} $C_{2,6}H$–$C_{3,5}H$ NOE cross-peak become less significant as the percentage of bound peptide increases. As both the decay rate of zero-quantum cross-peaks ($1/T_2{}^{(0)*}$) and the cross-relaxation rate are sensitive to τ_c (Macura et al., 1981, 1982), a possible explanation of the above results is that the C-terminus of the [D-Ala^9] analogue is constrained to a greater extent than that of the [L-Ala^9] peptide when both are in the bound state.

DISCUSSION

The [D-Ala^9]- and [L-Ala^9]α-factor analogues are linear peptides and are expected to be highly flexible in solution. Both the temperature coefficients for most residues (Table III) and the $^3J_{\alpha NH}$ coupling constants obtained for these peptides are consistent with conformational averaging. Although coupling constants are difficult to interpret when conformational averaging is present, the r^{-6} dependency of the nuclear Overhauser effect has been utilized to support the presence of transient species (Amodeo et al., 1991). Thus, the strong Pro$^8{}_{\alpha CH}$–Ala$^9{}_{NH}$ and Ala$^9{}_{NH}$–Gln$^{10}{}_{NH}$ cross-peaks and the weak Ala$^9{}_{\alpha CH}$–Gln$^{10}{}_{NH}$ cross-peak observed for the [D-Ala^9]α-factor in DMSO and water support the presence

of a transient type II β-turn centered about Pro^8 and Ala^9. In water the type II β-turn is further supported by the low-temperature coefficient of the Gln^{10} NH (–3.6 ppb/K) and the fact that the $Ala^9{}_{NH}$–$Gln^{10}{}_{NH}$ connectivity is the only cross-peak present in the NH–NH region of the [D-Ala^9] peptide.

The intensity of the $Ala^9{}_{NH}$–$Gln^{10}{}_{NH}$ cross-peak in the NOESY spectra of the [D-Ala^9]α-factor in DMSO (Figure 6A) supports the conclusion that the peptide adopts a type II β-turn conformation in this solvent. However, nearly all possible sequential NH–NH connectivities appear in the NOESY spectrum of the [D-Ala^9]α-factor in DMSO, and the temperature coefficient for the Gln^{10} NH resonance of the [D-Ala^9] analogue in DMSO (–3.3 ppb/K) is significantly higher than coefficients reported for strongly hydrogen bonded amide resonances in this solvent (Kessler, 1982; Balaram, 1985). This suggests either that the type II β-turn is less populated in this solvent (Amodeo et al., 1991) or that in DMSO the hydrogen bond is less important for the stability of the β-turn conformation. The presence of nearly all NH–NH connectivities in the NOESY spectrum of the [D-Ala^9] peptide in DMSO is probably the result of the longer effective correlation times in this solvent compared to that in water. The absence of nonsequential NOE connectivities together with the comparatively strong αCH_i–NH_{i+1} intensities precludes the correlation of these NH–NH connectivities with α-helical or other compact conformations. Similar results were observed in DMSO for the **a**-mating factor, which was determined to be a predominantly unstructured peptide in this solvent (Gounarides et al., 1991). The type II β-turn also appears to be the dominant conformation for the lipid-bound [D-Ala^9] analogue as judged by the strong $Pro^8{}_{\alpha CH}$–$Ala^9{}_{NH}$ and weak $Ala^9{}_{\alpha CH}$–$Gln^{10}{}_{NH}$ TRNOESY cross-peaks. The possibility that other conformers, with different internal mobilities, contribute to the observed TRNOE signal does not allow conclusions to be made as to whether the lipid stabilizes the β-turn conformation.

The [L-Ala^9]α-factor does not exhibit NMR parameters consistent with a regular secondary structure in DMSO or water or in the lipid-bound state. Both the absence of the $Met^{12}{}_{\alpha CH}$–$Tyr^{13}{}_{NH}$ cross-peak in the 400-ms NOESY spectrum of this peptide in aqueous solution and the increase in this TRNOE with peptide binding indicate that the C-terminus of the [L-Ala^9]α-factor has a shorter effective correlation time than does the C-terminus of the [D-Ala^9]α-factor analogue. In solution this result is consistent with the [L-Ala^9]α-factor being less structured than the [D-Ala^9]α-factor analogue. For both peptides binding to the lipid is strongest for the N-terminal residues. The C-terminal residues of the [L-Ala^9]α-factor do not appear to be directly involved in binding. In contrast, the mobilities of the C-terminal residues of the [D-Ala^9]α-factor are affected to a greater extent by the interaction with lipid vesicles. The disappearance of the $Met^{12}{}_{\alpha CH}$–$Tyr^{13}{}_{NH}$ cross-peak in the 8 mM DPPC/2 mM peptide spectrum on the [D-Ala^9]α-factor indicates that the mobility of this residue is more constrained in the lipid-bound state than residues 6–12 and suggests that the Tyr^{13} directly binds to the lipid. This result is consistent with the adoption of a compact conformation by the [D-Ala^9]α-factor.

We do not observe any of the nonsequential NOE connectivities that were reported by Jelicks et al. (1989). We attribute this to the following: (1) Chain-perdeuterated lipid was used in the present study, which minimized magnetization transfer (spin diffusion) through the lipid. (2) The experiments performed in this study were carried out using a much shorter mixing time [75 ms compared to 400 ms used by Jelicks et al. (1989)], which also reduced possible spin diffusion.

In conclusion, on the basis of NOE connectivities and temperature coefficients residues 7–10 of the [D-Ala^9]α-factor analogue exhibit a significant preference for a type II β-turn in solution and in the lipid-bound state, while the [L-Ala^9]α-factor analogue appears to be predominantly unstructured. The findings of this study support the conclusions of Jelicks et al. (1988, 1989) that a type II β-turn conformation spanning residues 7–10 is correlated with the activity of the mating factor.

It may be particularly significant that the [D-Ala^9]α-factor retains the type II β-turn in lipid, whereas the [L-Ala^9] homologue is unstructured under membrane-simulating conditions. A number of investigators have suggested that during the process of peptide-receptor recognition, interaction of the peptide with the membrane lipid facilitates the assumption of the biologically active conformation (Deber & Benham, 1985; Sargent & Schwyzer, 1986). Recent studies from our laboratory have also shown that α-factor analogues containing covalent constraints in the Lys-Pro-Gly-Gln region, which force the peptide to be bent about the Pro-Gly residues, retain significant biological activity and exhibit NMR parameters consistent with a β-turn (Xue et al., 1989; Naider et al., 1992). In all cases examined to date, analogues that can assume a type II β-turn have the highest biological activity. Thus, the findings in this paper, combined with biological data from a variety of mating factor analogues, support the notion that when the α-factor is bound to the receptor in the yeast cell membrane, it may be bent about the center of the pheromone.

However, the type II β-turn is apparently not the only factor important for α-factor activity. The N-terminal residues seem to play a significant role in binding to, and the triggering of, the receptor. Specifically, although the des-Trp^1[Cha^3,L-Ala^9] dodecapeptide was more than 200-fold less active than the corresponding D-homologue (Shenbagamurthi et al., 1985), the [L-Ala^9]α-factor is only 10-fold less active than the [D-Ala^9]α-factor. Both dodecapeptide and tridecapeptide analogues are expected to have similar conformational preferences. Furthermore, the findings that the des-Trp^1-[Ala^3]- and des-Trp^1[Phe^3]α-factor analogues are inactive but do compete with α-factor binding also suggest that the N-terminal residues play an important role in signal transduction by the receptor (Raths et al., 1988). Finally, in contrast to the conclusions of Higashijima et al. (1979) for the α-factor in solution and of Wakamatsu et al. (1986b) for α-factor in the presence of lipid vesicles, we find no evidence for a prevalent conformation other than the type II β-turn.

ACKNOWLEDGMENT

We are grateful to Dr. Michael Blumenstein and Professor Ruth Stark for their helpful comments. We gratefully acknowledge RCMI Grant 5G12RR03037-07, which supports the CUNY NMR facility.

REFERENCES

Allerhand, A., & Oldfield, E. (1973) *Biochemistry 12*, 3428–3433.

Amodeo, P., Motta, A., Picone, D., Saviano, G., Tancredi, T., & Temussi, P. A. (1991) *J. Magn. Reson. 95*, 201–207.

Balaram, P. (1985) *Proc. Indian Acad. Sci. (Chem. Sci.) 95*, 21–38.

Bax, A., & Davis, D. G. (1985) *J. Magn. Reson. 63*, 207–213.

Behling, R. W., Yamane, T., Navon, G., Sammon, M. J., & Jelinski, L. W.(1988) *Biophys. J. 53*, 947–954.

Campbell, A. P., & Sykes, B. D. (1991) *J. Magn. Reson. 98*, 77–92.

Chan, S. I., Sheetz, M. P., Seiter, C. H. A., Fergenson, G. W., Hsu, M.-C., Lau, A., & Lau, A. (1973) *Ann. N.Y. Acad. Sci. 222*, 499–522.

Clore, G. M., & Gronenborn, A. M. (1982) *J. Magn. Reson. 48*, 402–417.

Deber, C. M., & Benham, B. A. (1985) *Biopolymers 24*, 105–116.

de Kruijff, B., Cullis, R. R., & Radda, G. K. (1975) *Biochim. Biophys. Acta 406*, 6–20.

Dyson, J. H., Rance, M., Houghten, R. A., Lerner, R. A., & Wright, P. E. (1988) *J. Mol. Biol. 201*, 161–200.

Glaudemans, C. P. J., Lerner, L., Daves, G. D., Jr., Kováč, P., Venable, R., & Bax, A. (1990) *Biochemistry 29*, 10906–10911.

Gounarides, J. S., Xue, C., Broido, M. S., Becker, J. M., & Naider, F. (1991) *Biochem. Biophys. Res. Commun. 181*, 1125–1130.

Higashijima, T., Wakamatsu, K., Takemitsu, M., Fujino, M., Nakajima, T., & Miyazawa, T. (1983) *FEBS Lett. 152*, 227–230.

Higashijima, T., Masui, Y., Chino, N., Sakakibara, S., Kito, H., & Miyazawa, T. (1984) *Eur. J. Biochem. 140*, 163–171.

Jelicks, L. A., Naider, F. R., Shenbagamurthi, P., Becker, J. M., & Broido, M. S. (1988) *Biopolymers 27*, 431–449.

Jelicks, L. A., Broido, M. S., Becker, J. M., & Naider, F. R. (1989) *Biochemistry 28*, 4233–4240.

Kessler, H. (1982) *Angew. Chem., Int. Ed. Engl. 21*, 512–523.

Kumar, A., Wagner, G., Ernst, R. R., & Wüthrich, K. (1981) *J. Am. Chem. Soc. 103*, 3654–3658.

Macura, S., & Ernst, R. R. (1980) *Mol. Phys. 41*, 95–117.

Macura, S., Huang, Y., Suter, D., & Ernst, R. R. (1981) *J. Magn. Reson. 43*, 259–281.

Macura, S., Wüthrich, K., & Ernst, R. R. (1982) *J. Magn. Reson. 47*, 351–357.

Milon, A., Miyazawa, T., & Higashijima, T. (1990) *Biochemistry 29*, 65–75.

Mirau, P. A., & Bovey, F. A. (1986) *J. Am. Chem. Soc. 108*, 5130–5134.

Naider, F., Jelicks, L. A., Becker, J. M., & Broido, M. S. (1989) *Biopolymers 28*, 487–497.

Naider, F., Gounarides, J., Xue, C.-B., Bargiota, E., & Becker, J. M. (1992) *Biopolymers 32*, 335–339.

Neuhaus, D., & Williamson, M. (1989) in *The Nuclear Overhauser Effect in Structural and Conformational Analysis*, VCH Publishers, New York.

Otting, G., Widmer, H., Wagner, G., & Wüthrich (1985) *J. Magn. Reson. 66*, 187–193.

Rance, M., Sørensen, O. W., Bodenhausen, G., Wagner, G., Ernst, R. R., & Wüthrich, K. (1983) *Biochem. Biophys. Res. Commun. 117*, 479–485.

Raths, S. K., Naider, F., & Becker, J. M. (1988) *J. Biol. Chem. 263*, 17333–17341.

Rose, G. D., Gierasch, L. M., & Smith, J. A. (1985) *Adv. Protein Chem. 37*, 1–108.

Sargent, D. F., & Schwyzer, R. (1986) *Proc. Natl. Acad. Sci. U.S.A. 83*, 5774–5778.

Shenbagamurthi, P., Kundu, B., Raths, S., Becker, J. M., & Naider, F. (1985) *Biochemistry 24*, 7070–7076.

Sheetz, M. P., & Chan, S. I. (1972) *Biochemistry 11*, 4573–4581.

States, D. J., Haberkorn, R. A., & Ruben, D. J. (1982) *J. Magn. Reson. 48*, 286–292.

Stockton, G. W., Polnaszek, C. F., Tulloch, A. P., Hasan, F., & Smith, I. C. P. (1976) *Biochemistry 15*, 954–966.

Tallon, M. A., Shenbagamurthi, P., Marcus, S., Becker, J. M., & Naider, F. (1987) *Biochemistry 26*, 7767–7774.

Thorner, J. (1980) in *Molecular Genetics of Development: An Introduction to Recent Research on Experimental Systems* (Leighton, T. J., & Loomis, W. A., Jr., Eds.) pp 119–177, Academic Press, New York.

Valensin, G., Kushnir, T., & Navon, G. (1982) *J. Magn. Reson. 46*, 23–29.

Venkatachalam, C. M. (1968) *Biopolymers 6*, 1425–1436.

Wakamatsu, K., Okada, A., Higashijima, T., & Miyazawa, T. (1986a) *Biopolymers 25*, 193–200.

Wakamatsu, K., Okada, A., Suzuki, M., Higashijima, T., Masui, Y., Sakakibara, S., & Miyazawa, T. (1986b) *Eur. J. Biochem. 154*, 607–615.

Wakamatsu, K., Okada, A., Miyazawa, T., Masui, Y., Sakakibara, S., & Higashijima, T. (1987) *Eur. J. Biochem. 163*, 331–338.

Wright, P. E., Dyson, J. H., & Lerner, R. A. (1988) *Biochemistry 27*, 7169–7175.

Wu, C. S. C., Hachimori, H., & Yang, J. T. (1982) *Biochemistry 21*, 4556–4562.

Wüthrich, K. (1986) in *NMR of Proteins and Nucleic Acids*, Wiley, New York.

Xue, C.-B., Eriotou-Bargiota, E., Miller, D., Becker, J. M., & Naider, F. (1989) *J. Biol. Chem. 264*, 19161–19168.